Available online at www.sciencedirect.com
SCIENCE DIRECT®
Surface and Coatings Technology 183 (2004) 204–211
SURFACE & COATINGS TECHNOLOGY
www.elsevier.com/locate/surfcoat

Process-microstructure-property relationships in controlled atmosphere plasma spraying of ceramics

S. Beauvais[a], V. Guipont[a], F. Borit[a], M. Jeandin[a], M. Español[b], K.A. Khor[b,*], A. Robisson[c], R. Saenger[c]

[a]*Ecole Des Mines De Paris/C2P – Center for Plasma Processing, Evry, France*
[b]*Nanyang Technological University – School of Mechanical and Production Engineering, Singapore 639798, Singapore*
[c]*Schlumberger/Dept. Etudes et Production, Clamart, France*

Received 25 March 2003; accepted in revised form 19 August 2003

Abstract

Thermal plasma spray processes with their various operating parameters can be considered a flexible technique to carry out appropriate manufacturing of advanced ceramics coatings. This paper reports on investigations dealing with plasma spraying of several ceramics powders (hydroxyapatite, Al_2O_3–TiO_2, Al_2O_3, ZrO_2–Y_2O_3 (YSZ) and Cr_2O_3) with suitable parameters using a 'controlled atmosphere plasma spraying' (CAPS) system. High-pressure plasma spraying, air plasma spraying and inert plasma spraying modes were applied in order to obtain suitable microstructures in the coatings. The investigation of microstructures and phase compositions showed that high-pressure in the CAPS chamber leads to sufficient heating of the powder and have a promising coating quality.

Keywords: Plasma spray; Controlled atmosphere; Inert plasma spray; Advanced ceramics; Biomaterials; Microstructure

1. Introduction

The gas pressure surrounding the plasma plume has an effect on plasma properties, primarily the heating efficiency. In contrast with the processing of metals, the use of low pressures to reduce the coating porosity, is not suitable for high melting point materials such as ceramics because of the low heat capacity of the plasma. On the other hand, high pressures are expected to increase heat transfer from plasma to ceramic particles because of a higher volume density of plasma energy. The related heat transfer improvement can result in achieving dense coatings.

A so called 'high-pressure', i.e. of a few bars, decidedly shortens the plasma plume and concentrates the energy density within the high-pressure plasma spraying (HPPS) plasma [1–3]. Moreover, the use of an argon atmosphere promotes the heating capacity of the HPPS plasma jet. Argon gas ionises at a higher temperature (15 000 K) and is less energy-consuming than other atmospheres which exhibit lower dissociation temperature, e.g. nitrogen (7500 K) [4]. An earlier study also showed that HPPS can reduce porosity because of better heating of the powder and can therefore improve the thermo-mechanical properties of coatings [5].

The aim of this work is to ascertain the porosity reduction effect of HPPS for various sprayed ceramics (hydroxyapatite (HA), Al_2O_3–TiO_2, Al_2O_3, ZrO_2–Y_2O_3 and Cr_2O_3) to be applied to industrial components. The HPPS process, sprayed microstructures and specific properties (i.e. electric insulation, protection against liquid metal, coating lifetime,...) will be discussed. This provides material to initially establish process-microstructure-properties relationships for HPPS. In this work, the ceramic powders were sprayed using the HPPS, air plasma spraying (APS) and inert plasma spraying (IPS) modes in a controlled atmosphere plasma spraying (CAPS) system (Sulzer-Metco AG, Wohlen, Switzerland) [6].

2. Materials and processes

2.1. Substrates

Each substrate was selected in accordance to the specific application. For HA coatings the substrate was

*Corresponding author. Tel.: +65-790-5526; fax: +65-791-1859.
E-mail address: mkakhor@ntu.edu.sg (K.A. Khor).

0257-8972/04/$ - see front matter © 2003 Elsevier B.V. All rights reserved.
doi:10.1016/j.surfcoat.2003.08.078

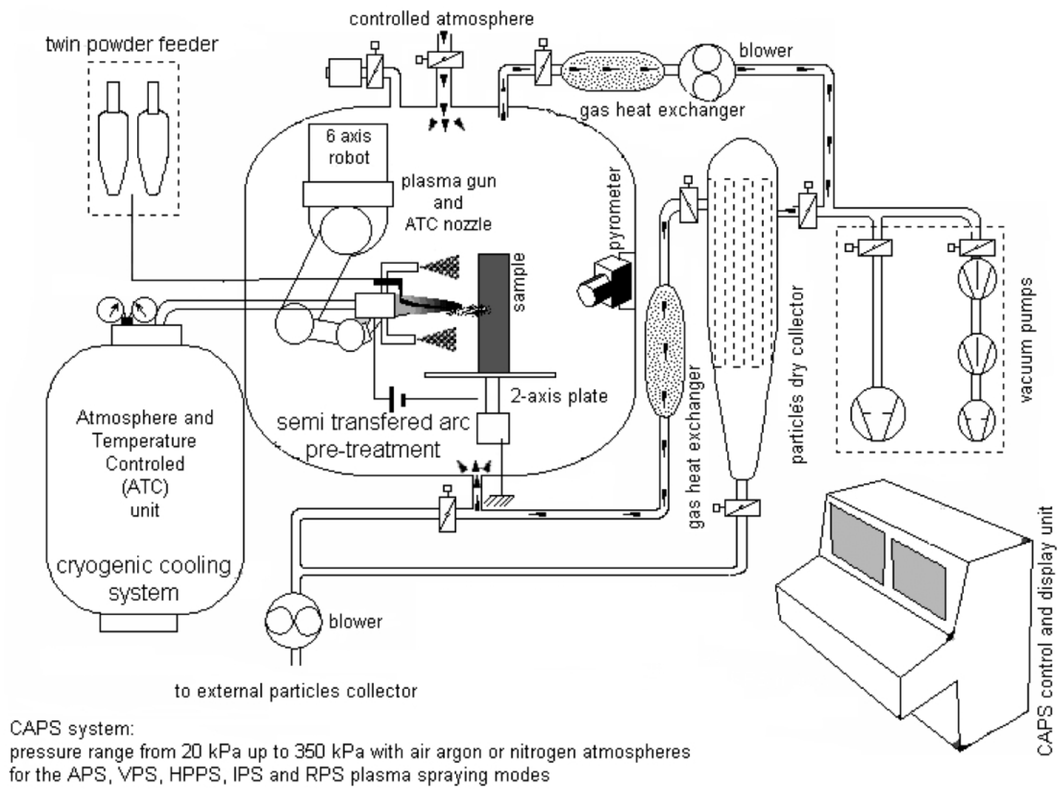

Fig. 1. Schematic illustration of the unit at the C2P.

Ti–6Al–4V, for alumina coatings it was 316 stainless steel and for YSZ and chromia it was conventional cast iron. The dimensions of substrates were as follows: Ti–6Al–4V: plates $25\times25\times2.5$ mm^3, steel: $25\times25\times2.5$ mm^3 and cast iron: cylindrical bars of 25 mm in diameter and 250 mm in length. All substrates were grit blasted before spraying. The grit-blasting procedure was operated using 300-μm alumina grit.

2.2. Powders

Commercial oxide powders were sprayed using CAPS with the particular aim to reduce the coating porosity. Al_2O_3–TiO_2 (METCO 101NS, $-45+11$ μm) and Al_2O_3 (METCO 105SFP, $-31+3.9$ μm) powders were used to develop coatings for electric insulation in an aqueous environment. Al_2O_3 (SNMI 22 SN012, $-45+20$ μm), YSZ (METCO 204NS, $-90+40$ μm) and Cr_2O_3 (AMDRY 6420, $-45+22$ μm) coatings were selected for protection of metallic rolls immersed in molten aluminum against metal erosion in an aqueous medium and hot corrosion. Non-commercial spherical HA powders (developed at NTU, Singapore [7]) were sprayed to study the microstructures and the phase compositions of bioactive coatings on metallic prostheses.

2.3. Spraying facilities

Spraying experiments were carried out using the CAPS system of the Center for Plasma Processing (C2P), ENSMP (Evry, France). It can operate in a controlled atmosphere of air, argon or nitrogen from 2 to 350 kPa. CAPS is a multi-process plasma equipment capable of spraying APS coatings (100 kPa, air), IPS coatings (100 kPa, argon) and VPS coatings (<100 kPa, air or argon) but also HPPS (in the 100–350 kPa pressure range) coatings. By extension, for example, when operating in a nitrogen atmosphere, reactive plasma spraying (RPS) can be coupled with HPPS [8,9]. During spraying, the CAPS atmosphere was cooled and recycled along with the removal of wasted particles through a closed loop including heat exchangers and dust collectors (Fig. 1).

3. HPPS plasma spraying

The ceramic powders were sprayed using the HPPS, APS and IPS modes. The atmosphere was air for APS, and argon for HPPS and IPS (Table 1). HPPS coatings were sprayed in a chamber of 18 m^3 using argon gas pressures of up to 250 kPa. Argon is more appropriate than air for the HPPS chamber atmosphere in order to avert nitric acid synthesis in the chamber during spraying when hydrogen is used as an auxilliary plasma gas.

To ensure optimized parameters, the powder jet deflection was measured prior to HPPS to keep the sprayed particles close to the center line of the plasma jet, thus ensuring optimized spray trajectory for the droplets in-flight. A small injector diameter of 1.1 mm was used to allow the powder to penetrate and cross a constricted and denser plasma jet due to high-pressure. Powder jet deflection through the plasma jet was measured for APS, IPS and HPPS. The carrier gas flow rates were calculated (with linear fitting, see Fig. 2) to satisfy the targeted value for deflection which was 3.5°, as usual for ceramic materials [10].

The plasma torch was a 50 kW d.c. 'Sulzer-Metco F4-MB' (nozzle internal diameter: 6 mm). Two different nozzles were used for air (for APS) or argon (for IPS and HPPS) cooling of the substrate during spraying. Plasma gas flow rates and electric efficiencies were selected to meet requirements for spraying using a conventional F4 plasma gun surrounded by an argon atmosphere of up to 250 kPa in order to reach comparable plasma power values as APS.

Nevertheless, as mentioned in an earlier work [5], with the employment of high-pressure in a CAPS chamber, some damage to the nozzle may occur when the HPPS power exceeds a certain limit. For high melting temperature materials like ceramics, a plasma gas mixture with a rather high H_2 content and moderate total plasma gas flow rate as conventionally used in APS is deemed not suitable for HPPS. It is hence necessary to drastically reduce the H_2 content in the Ar–H_2 plasma gas mixture. Different conditions were studied by Sodeoka et al. [11], varying arc intensities, nozzle diameters, plasma gas mixtures and flow rates. Measured heat losses through water-cooled nozzles are also higher due to heat concentration close to the electrode. To minimize cooling losses in the nozzles and the wear of the electrodes, a high plasma gas flow rate and addition of helium gas to increase the thermal efficiency of the plasma [12] were studied. Thorough preliminary experimental work, which is not discussed in this article, different spraying conditions with several binary Ar/H_2 and ternary Ar/H_2/He plasmas have been satisfactorily selected.

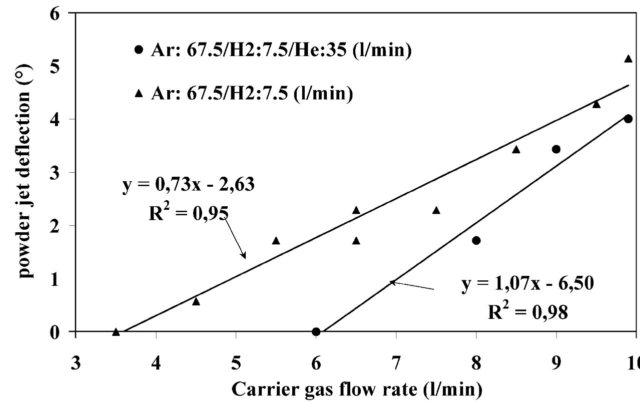

Fig. 2. Powder deflection vs. carrier gas flow rate.

4. Results and discussion

Five types of CAPS coatings were investigated.

4.1. Bioceramic hydroxyapatite coatings

Plasma spraying of bioceramic HA is performed to deposit bioactive coatings on prosthetic implants with

Table 1
Summary of CAPS modes and plasma gases (in l/min) used for ceramics

<table>
<tr><th>CAPS mode
pressure
atmosphere</th><th>APS
100 kPa
air</th><th>IPS
100 kPa
argon</th><th>HPPS
150 kPa
argon</th><th>HPPS
200 kPa
argon</th><th>HPPS
250 kPa
argon</th></tr>
<tr><td>Hydroxyapatite</td><td colspan="5">Ar:57 He:18 (no hydrogen)</td></tr>
<tr><td>Al_2O_3-TiO_2 3%</td><td colspan="3">Ar:38 H_2:9</td><td></td><td>Ar:67.5 H_2:7.5
Ar:67.5 H_2:7.5 He:35</td></tr>
<tr><td>Al_2O_3, fine</td><td colspan="2">Ar:41 H_2:14</td><td></td><td></td><td>Ar:67.5 H_2:7.5
Ar:67.5 H_2:7.5 He:35
Ar:67.5 H_2:1.5 He:15
Ar:67.5 H_2:1.5 He:35</td></tr>
<tr><td>Al_2O_3, medium</td><td>Ar:12 H_2:10 He:18</td><td></td><td></td><td></td><td>Ar:67.5 H_2:7.5 He:35</td></tr>
<tr><td>ZrO_2-Y_2O_3 8%</td><td>Ar:28 H_2:8</td><td></td><td></td><td></td><td>Ar:67.5 H_2:7.5 He:35</td></tr>
<tr><td>Cr_2O_3</td><td>Ar:33 H_2:13</td><td></td><td></td><td></td><td>Ar:67.5 H_2:7.5 He:35</td></tr>
</table>

Table 2
Plasma spraying parameters for CAPS HA coatings

Substrate	Grit blasted Ti–6Al–4V				
HA powder	HA 20–75 μm				
CAPS mode	APS	IPS	HPPS	HPPS	HPPS
Pressure (kPa)	100	100	150	200	250
Atmosphere	Air	Ar	Ar	Ar	Ar
Carrier gas flow rate (l/min)	5.9	4.4	5.5	6.6	7.7
Spraying distance	100 mm				
Powder feed rate	8 g/min				
Torch speed	1250 mm/s				
Pre-heating	120–150 °C				
Cooling of the substrate	Yes				

concomitant biocompatible and satisfactory mechanical properties. This study used exactly the same composition, the same flow rate (i.e. Ar–He) for the plasma gas mixture and the same degree of powder deflection for all spraying experiments, in the high-pressure mode as well as the atmospheric pressure (i.e. APS and IPS) modes (Table 1). The HPPS mode with three different pressures up to 250 kPa, APS and IPS modes were applied to assess pressure and atmosphere effects on HA coatings characteristics [13]. CAPS spraying parameters for spray-dried HA powder are given in Table 2.

The influence of the surrounding gas pressure was established by evaluating both CAPS HA coating microstructure and crystallinity, which are key properties for the manufacturing of reliable bioceramic coatings. Plasma-sprayed HA microstructure showed a positive correlation with the energy transfer from plasma to sprayed particles, i.e. especially the heating efficiency from the HPPS plasma plume that improves melting of the droplets. Consequently, the density of the HA coatings increased (Fig. 3 [13]). This corresponded with a better contact of the lamellae when a high-pressure (200 kPa) is applied in the CAPS chamber.

Figs. 4 and 5 show a high magnification scanning electron micrographs of the cross-sections of etched (5 s in diluted nitric acid) CAPS HA coatings sprayed in

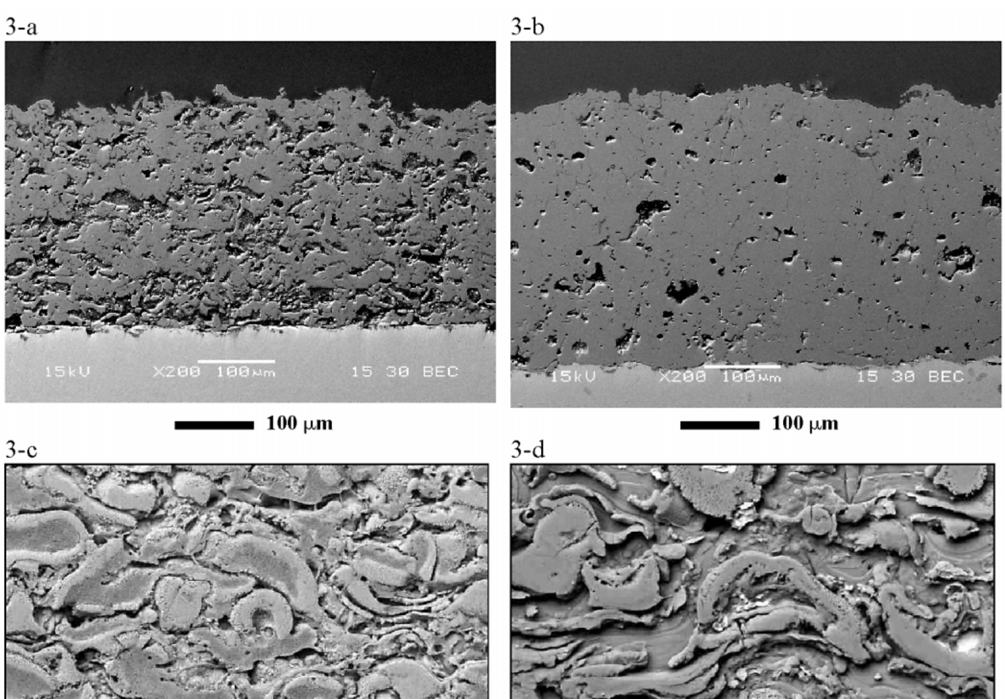

Fig. 3. Cross-section SEM view of CAPS HA coatings: (a) APS 100 kPa, air; (b) HPPS 200 kPa, argon; (c) *idem* 3-a after chemical etching and (d) *idem* 3-b after chemical etching.

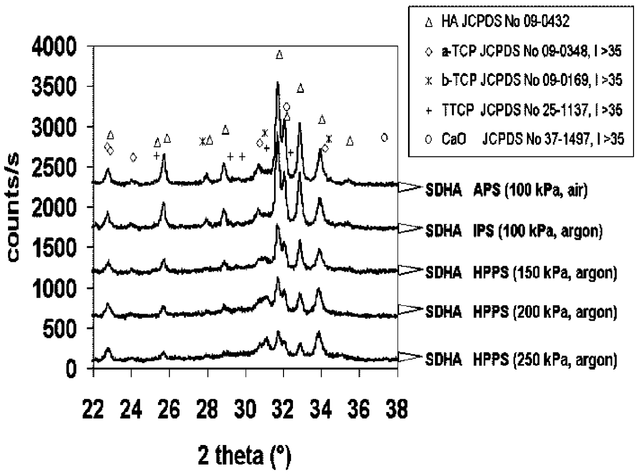

Fig. 4. XRD profiles (Cu Kα radiation) of CAPS HA coatings (after [13]).

the APS (100 kPa, air) and HPPS (200 kPa, argon) modes, respectively. Chemical etching preferentially removes amorphous material and reveals the coating structure. APS (100 kPa, air) HA particles were poorly melted and surrounded by thin amorphous boundaries, whereas the HPPS (250 kPa, argon) HA coating shows large, continuous and dense etched areas corresponding to a high amorphous phase content. The latter HA coating exhibited a pronounced lamellar structure that could play an important role for the enhancement of cohesion, mechanical properties and adhesion of the HA coating. On the contrary, the agglomerated microstructure of HA particles for APS HA coatings would lead to inferior mechanical properties.

Regarding the biological response of such as-sprayed HA coatings, the phase composition determined through XRD analyses showed a gradual and continuous amorphization of HA with increasing CAPS chamber pressure (Fig. 4). Ancillary calcium phosphate phases, i.e. tetracalcium phosphate and/or tricalcium phosphate (α-TCP, β-TCP), could be detected but in very small amounts in the coating. No CaO was found with XRD technique. This was verified by Fourier transform infrared spectrometry analyses [13]. HPPS HA coatings consisted mainly of amorphous phase and oxyhydroxyapatite (which is an intermediate phase of crystallized HA with gradual OH groups depletion when affected by high temperature). Coatings with the highest amorphous content were prepared at the highest CAPS chamber pressure (250 kPa).

Subsequent in vitro investigation revealed that the amorphous phase dissolves rapidly, which is perceived to impair formation of duration bonds with bony tissues. However, rapid dissolution may promote fast bone ingrowths and a speedy recovery for the patient if necessary. Therefore, CAPS process conditions that allow the build-up of HA deposits with strictly controlled and reproducible amorphous content *sans* CaO is indeed promising. It is also possible to adjust 'in vivo' dissolution behaviour by tailoring the phase composition and density of the thermal sprayed coating to promote appropriate and desirable properties in the bioactive HA.

4.2. Alumina–titania coatings

Alumina–titania (Al_2O_3–TiO_2) plasma-sprayed onto a metallic substrate is being studied to develop ceramic coating with good electric insulating properties in a very aggressive environment. The ceramic powder was sprayed using HPPS (150 and 250 kPa), APS and IPS

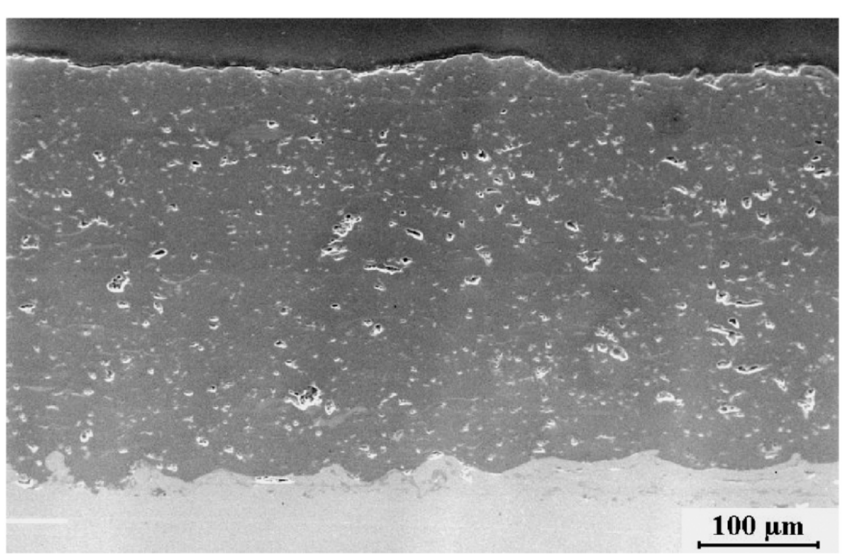

Fig. 5. SEM cross-sectional view of Al_2O_3–TiO_2 coating (with an APS NiCrAlY bond coat), HPPS at 250 kPa, Ar, 67.5 l/min; H_2, 7.5 l/min; He, 35 l/min, spraying distance of 100 mm.

Table 3
Thickness of Al_2O_3–TiO_2 plasma-sprayed coatings using different modes in CAPS

CAPS mode	Plasma	Spraying distance (mm)	Thickness (μm)
APS	Ar/H_2	130	270
IPS	Ar/H_2	130	300
HPPS (150 kPa)	Ar/H_2	130	330
HPPS (250 kPa)	Ar/H_2	130	240
HPPS (250 kPa)	$Ar/H_2/He$	130	330
HPPS (250 kPa)	Ar/H_2	100	270
HPPS (250 kPa)	$Ar/H_2/He$	100	375
HPPS (250 kPa)	Ar/H_2	200	120
HPPS (250 kPa)	$Ar/H_2/He$	200	210

(Table 1). All experiments were carried out with identical powder feed rate (30 g/min), powder deflection and spray duration (as determined by the number of strokes executed by the robotic manipulator arm). The relative deposition efficiency of the resulting coatings could be determined through coating thickness measurements (Table 3).

A NiCrAlY bond coat was sprayed in APS mode before spraying alumina–titania to enhance adhesion of the coatings.

The same plasma gas mixture ($Ar:H_2 = 38:9$ SLPM) was used for APS, IPS and HPPS (150 kPa). No significant difference, as far as thickness and microstructure were concerned, could be observed. This shows that the heatability of the plasma does not change significantly with a 'low' high-pressure and/or with an argon atmosphere.

One binary Ar/H_2 and one ternary $Ar/H_2/He$ plasma were studied with a 250-kPa pressure. The thickest coating was deposited using the shortest spray distance (100 mm instead of 130 mm for APS) and with a ternary plasma gas mixture ($Ar:H_2:He = 67.5:7.5:3.5$ SLPM) (Fig. 5).

The sole influence of pressure on microstructures cannot be discussed here because the plasma conditions were not the same for APS and HPPS. Resistance measurements, carried out in dry atmosphere at SCHLUMBERGER, showed that HPPS coatings can be more insulating than classical APS coatings by at least one order of magnitude (Fig. 6).

4.3. Alumina coatings

The spraying of pure alumina (Al_2O_3) was also studied to achieve electric insulation. Basically, alumina was expected to be a better insulator than alumina–titania due to the higher intrinsic resistivity of alumina. Alumina powder was sprayed using HPPS (four different plasmas at 250 kPa), APS and IPS modes. The microstructures were examined by SEM with a back-scattering electron detector (BSE), which was suitable for revealing the microstructure with a good contrast and without charge effects.

For HPPS coating using Ar(73.5 l/min)/H_2(1.5 l/min)/He(15 l/min) plasma, the reduction of the H_2 in the plasma content was not sufficiently balanced by the increase of He. Heat transfer was not good enough to melt all the powder. The microstructure shows a lot of unmelted feed particles in the coating and a rather high resulting porosity.

All the other coatings exhibited a conventional microstructure in which the porosity was low and homogenous. Globular pores due to incomplete spreading of droplets and line-shaped voids due to imperfect bonding between splats could be observed. Microcracks due to thermal stresses in the coatings did exist but were not detrimental for the coating quality (Fig. 7a and b).

The coating crystallographic phases were determined by X-ray diffraction (Fig. 8). These coatings contain some equilibrium α phase in addition to the metastable γ phase. The α-Al_2O_3 starting particles melted in the plasma plume. The undercooling of the resulting liquid droplets led to the nucleation of γ-Al_2O_3 nucleated rather than of α-Al_2O_3. Cooling rate after solidification was rapid enough to prevent subsequent transformation to α-Al_2O_3. The presence of α-Al_2O_3 in the coating was only due to the incorporation of unmelted α-Al_2O_3 particles. Diffraction patterns showed that the γ phase is the major phase in the coating. This indicates that the HPPS was efficient enough to heat the feedstock powder and that the injection of the powder was good and set a good trajectory of the particles.

Considering that all the experiments were carried out with the same powder feed rate (20 g/min), the same spray distance (130 mm), the same powder deviation and the same spraying time, the fact that the thickest coatings were obtained with HPPS plasmas seems to indicate that these spray conditions improved the heat transfer between the plasma and the particles. The deposition efficiency was, therefore, higher. These observations show that HPPS allows for achieving nearly dense alumina coatings.

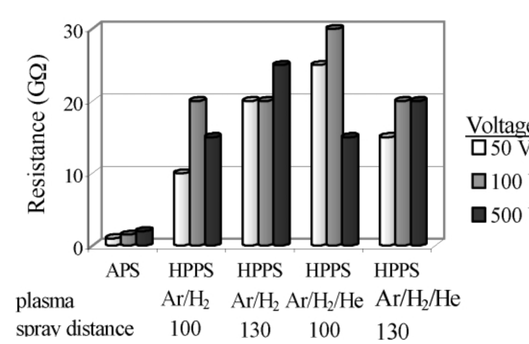

Fig. 6. Electric resistances in dry atmosphere of plasma-sprayed Al_2O_3–TiO_2 coatings for different CAPS modes (250 kPa).

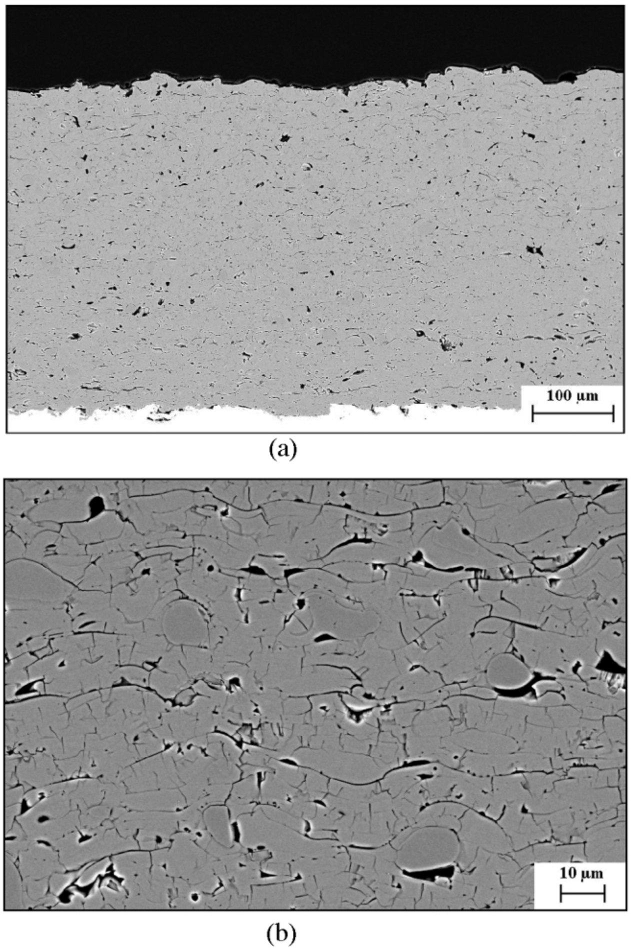

Fig. 7. SEM (BSE) cross-sectional view of Al_2O_3 coatings using HPPS (250 kPa, Ar, 67.5 l/min; H_2, 7.5 l/min; He, 35 l/min).

Three powder size distributions, namely, coarse: −90 +40 μm; medium: −45+20 μm and fine: −31+3.9 μm, were tested with satisfactory results. The grain size distribution of the feedstock powder is, therefore, not a restriction for the HPPS process.

4.4. Zirconia and chromia coatings

Yttria-stabilized-zirconia and chromia feedstock powders were sprayed in the HPPS mode at a pressure of 250 kPa to study the protection of cast iron rolls against liquid aluminum during aluminizing of steel. The resulting thermally sprayed chromia (Cr_2O_3) coating was investigated with SEM (Fig. 9). Porosity was low and homogeneously distributed. The presence of microcracks in the YSZ coating only showed that spraying temperature was rather elevated. A higher cooling during spraying would reduce residual stresses.

These coatings were tested in contact with liquid aluminum in an industrial setting. The coatings did not suffer any significant damage due to penetration/diffusion of liquid aluminum through the ceramic coating,

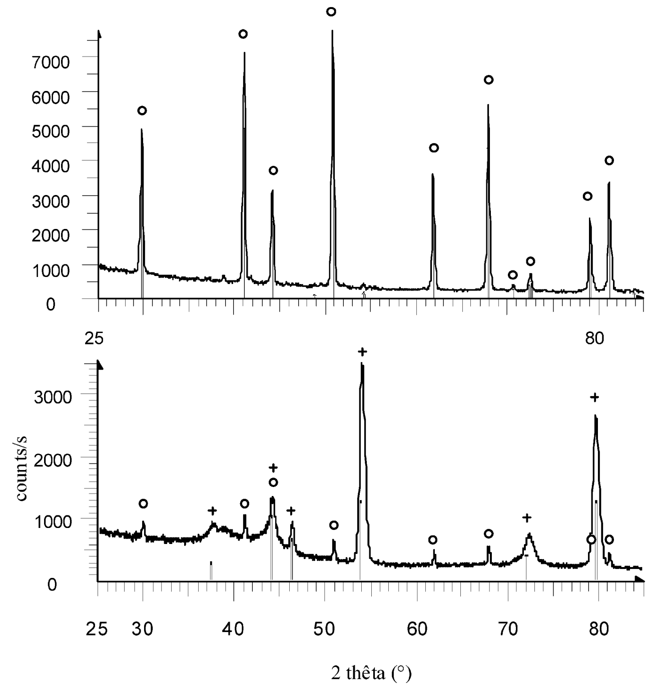

Fig. 8. XRD patterns (Co Kα radiation) of the METCO 105SFP alumina feedstock powder (top diagram) and of the resulting HPPS alumina coating (250 kPa, Ar, 67.5 l/min; H_2, 7.5 l/min) (bottom diagram); 'o' peaks correspond to α-Al_2O_3 and '+' peaks to γ-Al_2O_3.

which ascertains the potential use of HPPS-sprayed ceramics for this type of industrial application.

5. Conclusion

This study showed that HPPS could be successfully applied to a large range of ceramics. In most cases, the process was shown to lead to improved properties compared to conventional plasma-sprayed coatings. This is due to a better plasma-to-particles heat transfer under

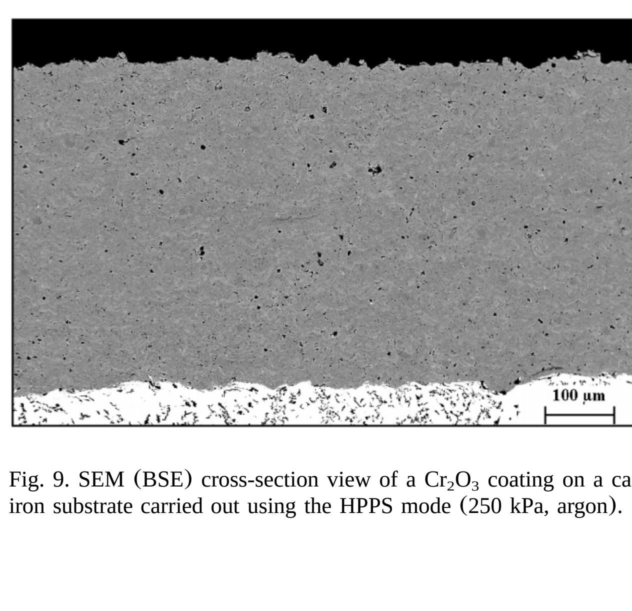

Fig. 9. SEM (BSE) cross-section view of a Cr_2O_3 coating on a cast iron substrate carried out using the HPPS mode (250 kPa, argon).

pressure that may result in reducing coating porosity and/or in better control of the coating microstructure.

HPPS was shown to be a reasonably versatile and flexible process, which does not require intricate procedures or equipment (e.g. a specific torch). Requirements for successful application are only a sound basic knowledge coupled with a certain know-how to both of which this study was expected to contribute. This highlights the role of plasma gas mixture composition, and of powder injection conditions in HPPS. Three examples of industrial applications of HPPS-sprayed ceramic coatings investigated were:

- biomedical applications, to obtain better-controlled microstructures that provide reliable performance and satisfy biological requirements, e.g. biocompatibility and bioactivity;
- oil industry applications, e.g. ceramic-coated formation resistivity sensors in oil well logging tools with higher insulating properties due to porosity reduction;
- steel-making industry applications, e.g. ceramic coatings to cast iron protect rolls from liquid metal attack due to their exceptionally low coating porosity and chemical inertness.

From the already existing background on HPPS, including the results of this study, one may think of RPS under pressure to promote 'in situ' reactions and resulting coatings. More basic further development should deal with investigation of porosity morphology and distribution. Since HPPS involves porosity in the low-value range, it is justified to study these aspects in current research work.

In conclusion, HPPS is undoubtedly an exciting source of new process-microstructure-property relationships, especially when applied to ceramics as shown in this study.

Acknowledgments

The authors would like to thank Dr Guesdon from USINOR-SOLLAC, Montataire, and Dr Choquet from USINOR-IRSID, Maizières-les-Metz, for financial support, helpful discussions and immersion testing of ceramic coatings. Mrs N. De Dave from the 'Ecole des Mines de Paris/C2P' is also gratefully acknowledged for technical assistance.

References

[1] D.A. Jager, D. Stöver, W. Schlump, High pressure plasma spraying in controlled atmosphere up to two bar, in: C.C. Berndt (Ed.), Thermal Spray: International Advances in Coatings Technology, ASM International, Materials Park, OH, USA, 1992, pp. 69–74.

[2] S. Sodeoka, M. Suzuki, T. Inoue, Y. Ono, K. Ueno, Plasma spraying under controlled atmosphere up to 300 kPa, in: A. Ohmori (Ed.), Thermal Spraying: Current Status and Future Trends, High Temperature Society of Japan, Osaka, Japan, 1995, pp. 283–288.

[3] T. Valente, L. Bertamini, M. Tului, Effect of pressure deposition on plasma jet and coatings microstructure, in: C.C. Berndt (Ed.), Thermal Spray/Practical Solutions for Engineering Problems, ASM International, Materials Park, OH, USA, 1996, pp. 463–470.

[4] M. Leylavergne, A. Vardelle, B. Dussoubs, Comparison of plasma sprayed coatings produced in argon or in nitrogen atmosphere, in: C.C. Berndt (Ed.), Thermal Spray: A United Forum for Scientific and Technological Advances, ASM International, Materials Park, OH, USA, 1997, pp. 459–465.

[5] S. Sodeoka, M. Suzuki, K. Ueno, J. Therm. Spray Technol. 5 (3) (1996) 277–282.

[6] S. Keller, M. Tommer, R. Clarke, A.R. Nicoll, Key factors in the development of plasma spray process, in: A. Ohmori (Ed.), Thermal Spraying: Current Status and Future Trends, High Temperature Society of Japan, Osaka, Japan, 1995, pp. 275–281.

[7] S.W.K. Kweh, K.A. Khor, P. Cheang, Biomaterials 21 (2000) 1223–1234.

[8] T. Eckardt, W. Mallener, D. Stöver, Reactive plasma spraying of silicon in controlled nitrogen atmosphere, in: C.C. Berndt, S. Sampath (Eds.), 1994 Thermal Spray Industrial Applications, ASM International, Materials Park, OH, USA, 1994, pp. 515–519.

[9] M. Suzuki, S. Sodeoka, T. Inoue, K. Ueno, T. Valente, Fabrication of Ti nitrides by reactive plasma spraying, in: E. Lugscheider, P.A. Kamer (Eds.) Proceedings of the United Thermal Spray Conference 99, 17–19 Mars 1999, DVS Verlag: Düsseldorf, Allemagne, 1999, pp. 265–270.

[10] M. Vardelle, A. Vardelle, P. Fauchais, J. Therm. Spray Technol. 2 (1) (1993) 79–91.

[11] S. Sodeoka, M. Suzuki, K. Ueno, Effect of spray parameters on the plasma in high pressure plasma spraying up to 300 kPa, in: C. Coddet (Ed.), Thermal Spray: Meeting the Challenges of the 21st Century, Materials Park, OH, USA: ASM International, 1998, pp. 1437–1441.

[12] S. Janisson, E. Meillot, A. Vardelle, J.F. Coudert, B. Pateyron, P. Fauchais, Plasma spraying using Ar–He–H_2 gas mixtures, in: C. Coddet (Ed.), Thermal Spray: Meeting the Challenges of the 21st Century, Materials Park, OH, USA: ASM International, 1998, pp. 803–808.

[13] V. Guipont, M. Espanol, F. Borit, N. Llorca-Isern, M. Jeandin, K.A. Khor, Mater. Sci. Eng. A 325 (2002) 9–17.